Hindawi
Advances in Materials Science and Engineering
Volume 2019, Article ID 8789151, 13 pages
https://doi.org/10.1155/2019/8789151

Research Article

A Stress Analysis of Some Fundamental Specimens of Soft-Matter Quasicrystals with Eightfold Symmetry Based on Generalized Dynamics

Fang Wang[1], **Hui Cheng**[2], **Tian-You Fan**[3] and **Hai-Yun Hu**[3]

[1]*School of Natural Science, Shuozhou Advanced Normal College, Shuozhou 036002, Shanxi Province, China*
[2]*School of Mathematical and Physical Science and Engineering, Hebei University of Engineering, Handan 056038, Hebei Province, China*
[3]*School of Physics, Beijing Institute of Technology, Beijing 100081, China*

Correspondence should be addressed to Tian-You Fan; tyfan2013@163.com

Received 28 August 2018; Revised 10 December 2018; Accepted 18 March 2019; Published 7 May 2019

Academic Editor: Zhiping Luo

This paper reports a stress analysis of some fundamental samples made of soft-matter quasicrystals with 8-fold symmetry based on the generalized dynamics. The most distinction from the hydrodynamics for solid quasicrystals is that the structure of soft matter belongs to a complex liquid, which is an intermediate phase between solid and liquid and behaves natures of both solid and liquid. In addition, the soft-matter quasicrystals possess high symmetry, and the symmetry breaking is of fundamental importance. So the Landau symmetry breaking theory and elementary excitation principle are therefore the paradigm of the study of soft-matter quasicrystals. Soft-matter quasicrystals belong to the complex fluid, in which the fluid phonon elementary excitation is introduced apart from the phonon and phason elementary excitations. With this model and the equation of state, the equations of motion for possible soft-matter quasicrystals of 8-fold symmetry are derived. The initial boundary value problems for the xy plane field are solved by applying the finite difference method, in which the z-direction represents the 8-fold symmetry axis. A complete hydrodynamics analysis is given to quantitatively explore the phonon, phason, and fluid fields as well as their interactions in the physical time-space domain. The analysis shows the governing equations are exact to the prediction of the dynamics of soft-matter quasicrystals. The computational results reveal the gigantic differences of physical properties between solid and soft-matter quasicrystals.

1. Introduction

Fan [1] suggested a theory of generalized hydrodynamics, or generalized dynamics in brief, for soft-matter quasicrystals observed in liquid crystals, colloids, and polymers during the period 2004–2011 [2–6] and in surfactants more recently [7] by analyzing and summarizing their symmetry, structure, and dynamic behaviour. The theory is inspired by the hydrodynamics of solid quasicrystals proposed by Lubensky et al. [8], but there are principal differences between the hydrodynamics of soft-matter and solid quasicrystals.

In the hydrodynamics of solid quasicrystals, the effects of solid viscosity and elasticity are considered, while in the hydrodynamics of soft-matter quasicrystals, the effects of fluid and elasticity are studied. Due to this difference, in the hydrodynamics of soft-matter quasicrystals, one should introduce the fluid phonon elementary excitation apart from the phonon and phason excitations in which the latter are well known in the solid quasicrystal study, and the fluid phonon is introduced for the first time by Fan [1] for the soft-matter quasicrystal study although which was originated from the Landau school [9], and they claimed that the fluid acoustic wave is a fluid phonon. In this case, the equation of state $p = f(\rho)$ for soft matter must be introduced, where p denotes the fluid pressure and ρ the mass density. It is well known that the equation of state of soft matter is a longstanding puzzle in the thermodynamic study. Based on the original Wensink's work [10], Fan [1] made some modifications to obtain a very simple and applicable equation of state, which will be given in the next section.

The present paper develops a mathematical method for solving the initial-boundary value problem of possible octagonal soft-matter quasicrystals. The numerical implementation of the method by using the finite difference approach is carried out, and systematical results are obtained. The method developed here is suitable for all quasicrystals of the first kind of soft-matter quasicrystals observed so far (or will be discovered in future), but here we only discuss the possible ones with 8-fold symmetry, which are more interesting than those with 12- and 18-fold symmetry. In the latter two classes of quasicrystals, which have already been observed experimentally, phonons and phasons are decoupled to each other, leading to possible missing of certain interesting physical properties. On the contrary, there is strong coupling between phonons and phasons in the quasicrystals with 8-fold symmetry, which may give rise to very important phenomena.

Though experimental data of soft-matter quasicrystals are still very few up to now, the study on some fundamental problems may be important. Through the study, some basic physical and mechanical properties can be explored, which will give guidelines for the future material characterization of soft-matter quasicrystals. In particular, the stress analysis is theoretically fundamental and of practical significance. In this paper, we are interested in the distribution, deformation, and motion of the matter induced by the applied stress field. The interaction between the elementary excitations (e.g., phonons, phasons, and fluid phonon) will be the core of this study. Relevant results exploring the intrinsic differences between soft-matter and solid quasicrystals will be given.

1.1. Equation System of Generalized Dynamics of Soft-Matter Quasicrystal with 8 mm Symmetry in Two Dimensions. Apart from the observed 12- and 18-fold symmetrical soft-matter quasicrystals and possible 5- and 10-fold symmetrical soft-matter quasicrystals, the 8-fold symmetrical soft-matter quasicrystals may also be observed in a near future. This kind of soft-matter quasicrystal is very stable and presents important meaning. Especially between phonons and phasons, there is strong coupling effect, and it is more interesting in the study of their mechanical and physical properties and mathematical solutions. If we consider the plane field in the xy plane and z-axis is 8-fold symmetry axis, the field components relating to variable z vanish, and all field variables are independent from z. As is shown in Figure 1, the specimen's center is placed at the coordinate system's origin, the x-axis is along the horizontal direction and the y-axis is along the perpendicular direction. The rectangular specimen is symmetric about the x-axis in the horizontal direction and symmetric about the y-axis in the perpendicular direction. Hence for the possible soft-matter octagonal quasicrystals, there is a final governing equation system of the generalized hydrodynamics [1]:

$$
\begin{aligned}
&\frac{\partial \rho}{\partial t} + \nabla \cdot (\rho \mathbf{V}) = 0,\\
&\frac{\partial (\rho V_x)}{\partial t} + \frac{\partial (V_x \rho V_x)}{\partial x} + \frac{\partial (V_y \rho V_x)}{\partial y} = -\frac{\partial p}{\partial x} + \eta \nabla^2 (\rho V_x) + \frac{1}{3}\eta \frac{\partial}{\partial x} \nabla \cdot (\rho \mathbf{V}) + M \nabla^2 u_x + (L + M - B) \frac{\partial}{\partial x} \nabla \cdot \mathbf{u}\\
&\qquad + R\left(\frac{\partial^2 w_x}{\partial x^2} + 2\frac{\partial^2 w_y}{\partial x \partial y} - \frac{\partial^2 w_x}{\partial y^2} \right) - (A - B) \frac{1}{\rho_0} \frac{\partial \delta \rho}{\partial x},\\
&\frac{\partial (\rho V_y)}{\partial t} + \frac{\partial (V_x \rho V_y)}{\partial x} + \frac{\partial (V_y \rho V_y)}{\partial y} = -\frac{\partial p}{\partial y} + \eta \nabla^2 (\rho V_y) + \frac{1}{3}\eta \frac{\partial}{\partial y} \nabla \cdot (\rho \mathbf{V}) + M \nabla^2 u_y + (L + M - B) \frac{\partial}{\partial y} \nabla \cdot \mathbf{u}\\
&\qquad + R\left(\frac{\partial^2 w_y}{\partial x^2} - 2\frac{\partial^2 w_x}{\partial x \partial y} - \frac{\partial^2 w_y}{\partial y^2} \right) - (A - B) \frac{1}{\rho_0} \frac{\partial \delta \rho}{\partial y},\\
&\frac{\partial u_x}{\partial t} + V_x \frac{\partial u_x}{\partial x} + V_y \frac{\partial u_x}{\partial y} = V_x + \Gamma_u \left[M \nabla^2 u_x + (L + M) \frac{\partial}{\partial x} \nabla \cdot \mathbf{u} + R\left(\frac{\partial^2 w_x}{\partial x^2} + 2\frac{\partial^2 w_y}{\partial x \partial y} - \frac{\partial w_x}{\partial y^2} \right) \right],\\
&\frac{\partial u_y}{\partial t} + V_x \frac{\partial u_y}{\partial x} + V_y \frac{\partial u_y}{\partial y} = V_y + \Gamma_u \left[M \nabla^2 u_y + (L + M) \frac{\partial}{\partial y} \nabla \cdot \mathbf{u} + R_1 \left(\frac{\partial^2 w_y}{\partial x^2} - 2\frac{\partial^2 w_x}{\partial x \partial y} - \frac{\partial^2 w_y}{\partial y^2} \right) \right],\\
&\frac{\partial w_x}{\partial t} + V_x \frac{\partial w_x}{\partial x} + V_y \frac{\partial w_x}{\partial y} = \Gamma_w \left[K_1 \nabla^2 w_x + (K_2 + K_3) \left(\frac{\partial^2 w_x}{\partial y^2} + \frac{\partial^2 w_y}{\partial x \partial y} \right) + R\left(\frac{\partial^2 u_x}{\partial x^2} - 2\frac{\partial^2 u_y}{\partial x \partial y} - \frac{\partial^2 u_x}{\partial y^2} \right) \right],\\
&\frac{\partial w_y}{\partial t} + V_x \frac{\partial w_y}{\partial x} + V_y \frac{\partial w_y}{\partial y} = \Gamma_w \left[K_1 \nabla^2 w_y + (K_2 + K_3) \left(\frac{\partial^2 w_x}{\partial x \partial y} + \frac{\partial^2 w_y}{\partial x^2} \right) + R\left(\frac{\partial^2 u_y}{\partial x^2} + 2\frac{\partial^2 u_x}{\partial x \partial y} - \frac{\partial^2 u_y}{\partial y^2} \right) \right],\\
&p = 3\frac{K_B T}{l^3} \left(\frac{\rho}{\rho_0} + \frac{\rho^2}{\rho_0^2} + \frac{\rho^3}{\rho_0^3} \right),
\end{aligned}
\tag{1}
$$

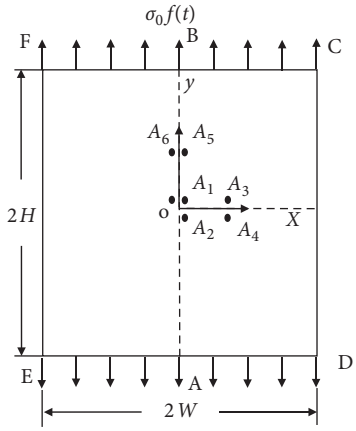

Figure 1: Specimen of soft-matter quasicrystals of 8-fold symmetry under dynamic loading.

where $\nabla \cdot \mathbf{u} = \mathbf{i}(\partial/\partial x) + \mathbf{j}(\partial/\partial y)$, $\nabla^2 = (\partial^2/\partial x^2) + (\partial^2/\partial y^2)$, and $\mathbf{u} = \mathbf{i}u_x + \mathbf{j}u_y$ represents phonon displacement vector, $\mathbf{w} = \mathbf{i}\omega_x + \mathbf{j}\omega_y$ the phason displacement vector, $\mathbf{V} = \mathbf{i}V_x + \mathbf{j}V_y$ the fluid velocity vector, $L = C_{12}, M = (C_{11} - C_{12})/2$ the phonon elastic constants, and K_1, K_2, and K_3 the phason elastic constants, R the coupling elastic constant between the phonon and phason fields, and η the fluid dynamic viscosity, respectively; for the details on constitutive law, refer to Appendix. The last equation in system (1) is the equation of state, which is the thermodynamic result of soft matter, and does not belong to the result of derivation of the pure hydrodynamics, in which ρ_0 denotes the initial value of mass density, K_B is the Boltzmann constant, T is the absolute temperature, l is the characteristic size of soft matter, in general is in 1~100 nm, and in the following computation, we take 8~9 nm and achieved best results.

2. Sample I, Fluctuation due to the External Stress

2.1. Statement of the Problem. The aim of this study lies in revealing the characters of deformation and motion of soft-matter quasicrystals from the point of view of hydrodynamics, and the equation (1) provides a basis for the analysis; the solving system of which in physical space-time domain is of same importance and otherwise one cannot get any worth information. First, only through the practical computation, the correctness, efficiency, and solvability of the equations can be verified. Second, the computation determines key field variables of the hydrodynamics of the matter, which provides the fundamental theoretical results and applicable data in experiments. For this purpose, a specimen made by the matter is designed as shown in Figure 1, and the corresponding initial- and boundary-value conditions are as follows:

$$t = 0, u_x = u_y = 0, w_x = w_y = 0, V_x = V_y = 0, p = f(\rho_0),$$
$$y = \pm H, |x| < W, V_x = V_y = 0, \sigma_{yy} = \sigma_0 f(t), \sigma_{yx} = 0,$$
$$H_{yy} = H_{yx} = 0, p = p_0,$$
$$x = \pm W, |y| < H, V_x = V_y = 0, \sigma_{xx} = \sigma_{xy} = 0, H_{xx} = H_{xy} = 0, p = p_0. \quad (2)$$

(3)

In the present computation, we take the relevant geometry parameters and material constants [11] as follows and assume the dynamic loading function $f(t)$ is the Heaviside [12] function of time: $2H = 0.01\,\text{m}, 2W = 0.01\,\text{m}, \sigma_0 = 0.01\,\text{MPa}$, $\rho_0 = 1.5 \times 10^3\,\text{kg/m}^3, \eta = 0.1\,\text{Pa·s}, L = 10\,\text{MPa}$ [13, 14], $M = 4\,\text{MPa}$ [15], $K_1 = 0.5\,\text{L}, K_2 = -0.1\,\text{L}, K_3 = 0.05\,\text{L}, R = 0.04\,\text{M}$, $\Gamma_u = 4.8 \times 10^{-17}\,\text{m·s/kg}, \Gamma_w = 4.8 \times 10^{-19}\,\text{m}^3\text{·s/kg}$. [16].

The initial boundary value problem of equations (2)-(3) with nonlinear partial differential equation (1) is consistent mathematically, but the existence and uniqueness of solution has not been proven from the theory of partial differential equations yet due to the complexity of the problem. We can solve it by the numerical method, and the stability and correctness of solution can be verified by the numerical results only.

2.2. Numerical Results. Here, we take a finite difference method for solving the above initial boundary value problem, and some results are given through the illustrations shown in Figures 2–7.

2.3. Analysis of Results. It is well known that the phonon represents wave propagation, while phason represents diffusion for solid quasicrystals and for soft-matter quasicrystals. In the soft-matter quasicrystals, there is another elementary excitation—fluid phonon, which represents the fluid acoustic wave propagation. The wave propagation dominates the physical process in the studied specimen, while the phonon and phason fields are coupled to each other.

The specimen shown in Figure 1 is subjected to a dynamic loading at the upper and lower surfaces, and the action of the outer field is equivalent to a wave emanated from the surfaces. Before the wave arrives at the plane located of computing point A_1 (or A_2), there is no any response of any field variables at the location, and this is the simplest and most important fact physically; all of our computational results prove the point. For example, from Figure 2(a), the wave emanated from the upper or lower surface propagating to point $A_1(10^{-4}\,\text{m}, 10^{-4}\,\text{m})$ (or $A_2(10^{-4}\,\text{m}, -10^{-4}\,\text{m})$) experiences $t_0 = 4.07 \times 10^{-5}\,\text{s}$. Its propagation distance is $H_0 = H - 10^{-4} = 0.0049\,\text{m}$; thus, the speed of the wave is $c = H_0/t_0 = 0.0049/4.07 \times 10^{-5} = 120.39\,\text{m·s}^{-1}$. Also we can see that the density of soft-matter quasicrystals in Figure 3(a) decreases to $\rho_{\min} = 1498\,\text{kg·m}^{-3}$ and the speed of the elastic longitudinal wave is $c_{\max} = \sqrt{(A + L + 2M - 2B/\rho_{\min})} = 109.6176\,\text{m·s}^{-1}$, which is very close to measured wave speed c; in fact, the error is only 0.006. Also the internal pressure decreases to $p_{\min} = 1.011 \times 10^5\,\text{Pa}$

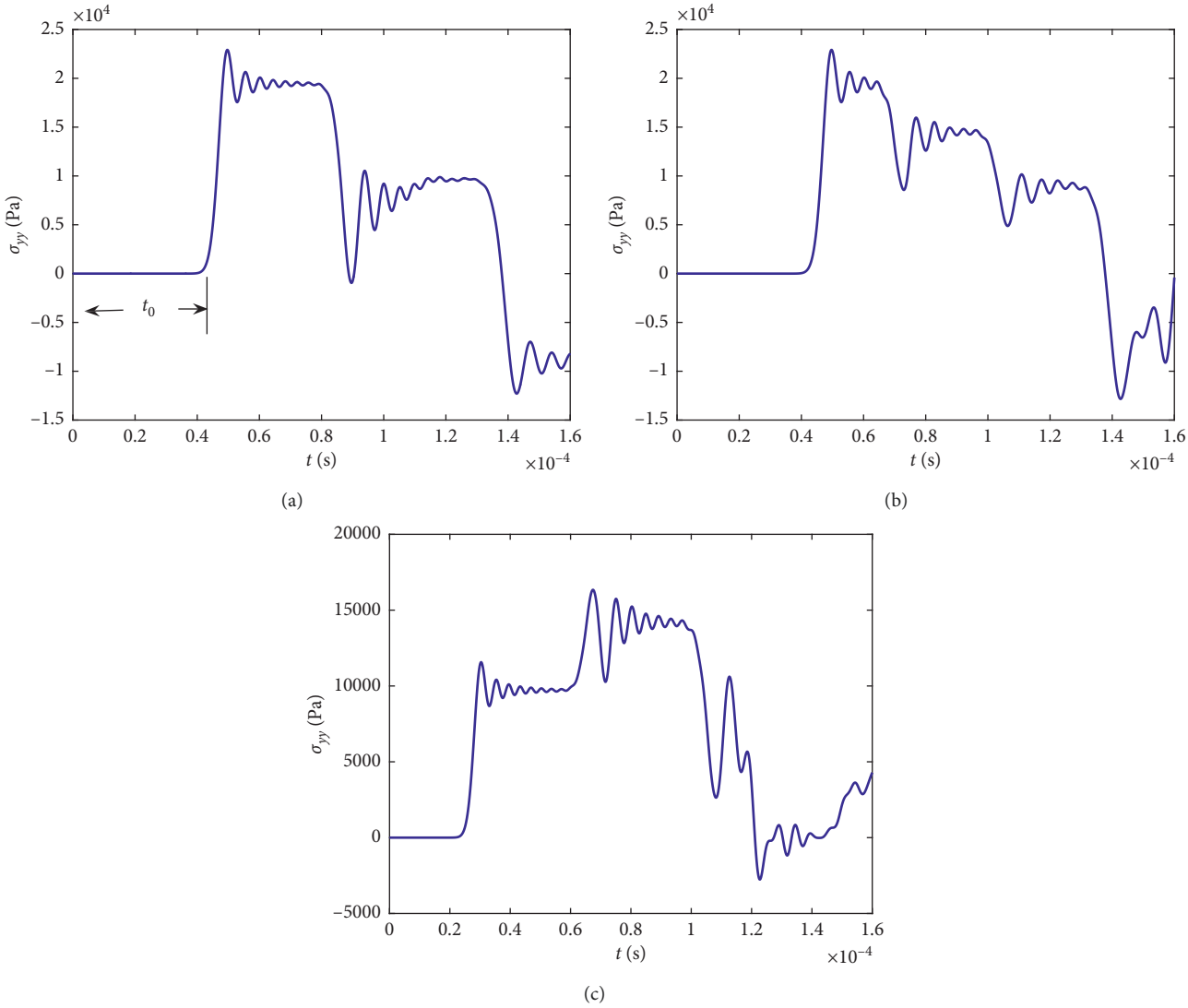

FIGURE 2: Normal stress of phonon field versus time (a) at the point A_1 (or A_2) of the specimen; (b) at the point A_3 (or A_4) 2 mm from A_1 (or A_2) towards the right in the horizontal direction; (c) at the point A_8 (or A_9) 2 mm from A_1 (or A_7) up in the perpendicular direction.

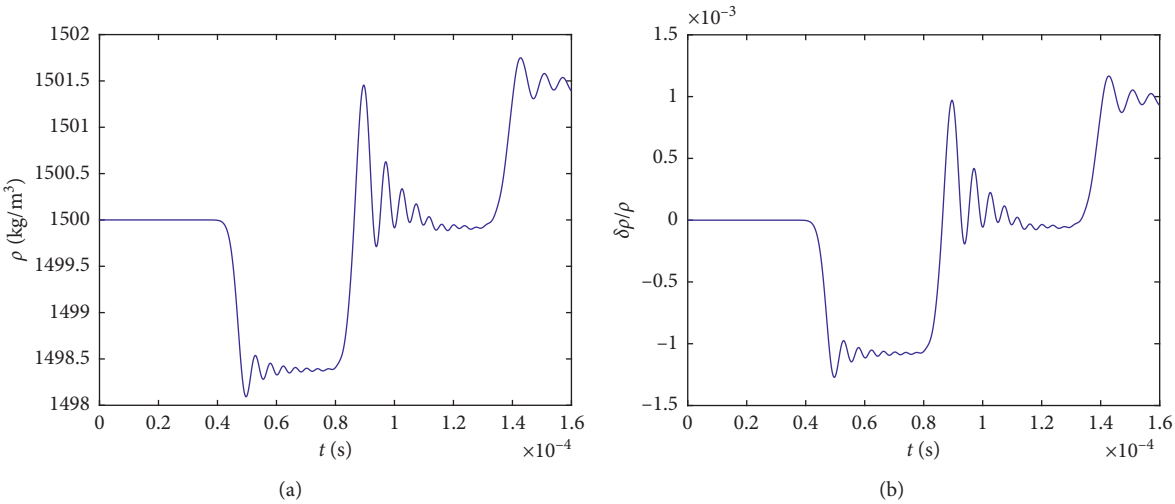

FIGURE 3: (a) Mass density at the point A_1 (or A_2) of the specimen versus time and (b) variation of mass density of the computational point A_1 (or A_2) of the specimen versus time.

(Figure 4). In the normal elastic solid matter, there is one longitudinal wave speed $c_1 = \sqrt{(A + L + 2M - 2B/\rho)} = 109.5445$ m/s. In addition, the speed of two elastic transverse speeds $c_2 = c_3 = \sqrt{M/\rho} = 51.6398$ m/s and the speed of fluid acoustic longitudinal $(c_4)_0 = \sqrt{\partial p/\partial \rho}\,|_{\rho=\rho_0} = 11.6232\ \mathrm{m\cdot s^{-1}}$ (Figure 5). Comparing to the above results, it is obvious that c_1 plays the dominated role although soft matter is an intermediate phase between solid and liquid, which has 4 kinds of waves. The above results examine the correctness of governing equations, initial- and boundary-value conditions, as well as the effectiveness of the numerical method and computer program from most fundamental physical fact.

Figures 2(a)–2(c) show the normal stress of the phonon field versus time, about the points A_1, A_3, and A_5. From the figures, we can see that the magnitude of the normal stress is almost equal, but the shapes of the waves are different. Further comparison of the results about A_1 and A_5 shows that the experienced time t_0 is not the same since the propagation distance from the upper to the point studied is not equal and the experienced time for A_5 is shorter than A_1 because the propagation distance is shorter. However, the experienced time of A_1 and A_3 is equal, it is easy to see that the propagation distance is equal from Figures 2(a) and 2(b).

In Figures 6(a)–(6c), the normal stress of the fluid phonon field varies versus time, the case is similar to the above results, and the experienced time depends on the propagation distance, so for A_1 and A_3, the experienced time is the same but is not for A_1 and A_5. Though the magnitude of the fluid phonon stresses is nearly equal, but the shapes of waves are also different for different points.

In Figures 7(a)–7(c), about the normal stress of the phason field versus time, of course for the same reason the case is similar too. Apart from Figures 2 and 6, the shape of figures reveals dissipation effects. Meanwhile, we find out that nearer to the boundary, such as for A_3 and A_5, the phason stresses have smaller vibrations than A_1.

Because A_3 and A_4 are symmetric about the x-axis, it is not hard to imagine the results are the same for the same kind of field. Also A_5 and A_6 are symmetric about the y-axis, and the results are the same too. On further promotion, the total sample is symmetric about the x- and y-axis, which enables us to understand that the points in negative axis are also symmetric to those points in the positive x- and y-axis; so the results of them are identical.

Moreover, a comparison of the above results with those for the solid quasicrystals (e.g., 5- and 10-fold quasicrystals in [12]) is necessary. The orders of the magnitude of the stresses such as σ_{yy} and H_{yy} for the soft-matter quasicrystals are the same to those for the solid quasicrystals. For example, the order of the magnitude of the phonon normal stress of the solid quasicrystal is 10^4, which is equal to those in Figure 2; at the same time, that of the phason stress of the solid quasicrystal is 10^2, which is also equal to those in Figure 7, although there is a little difference. So the effect of elastic is similar for both solid and soft-matter quasicrystals. In contrast to this, the order of the magnitude for the viscosity normal stress σ'_{ij} of the solid quasicrystal (the order is 10^{-10}) is much smaller than the fluid normal stress P_{ij} of soft-matter quasicrystals (the order is 10^5) in Figure 6. The

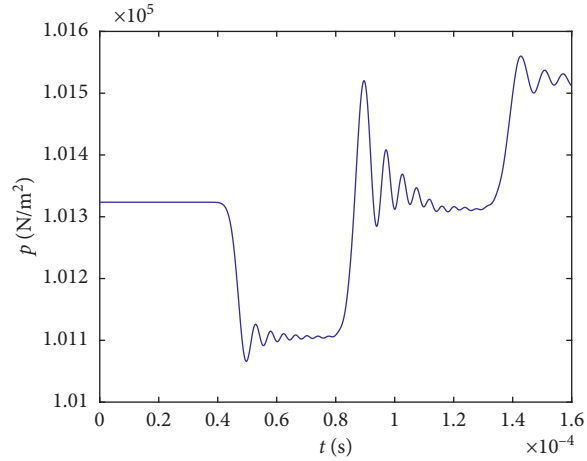

Figure 4: Fluid pressure at the point A_1 (or A_2) of the specimen versus time, reprinted from [11], copyright 2017 with permission from Springer Nature.

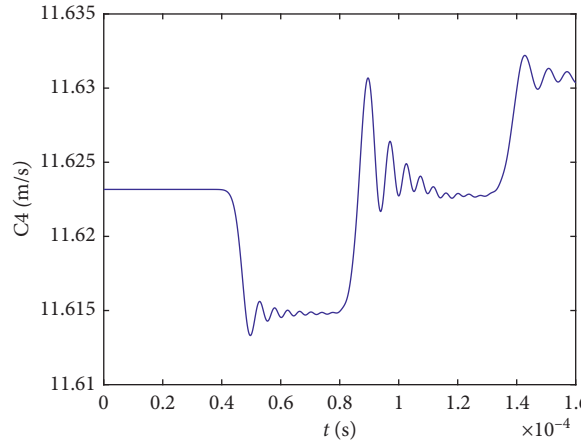

Figure 5: Velocity of the fluid acoustic wave at the point A_1 (or A_2) of specimen versus time.

reason is that the effect of solid viscosity is too weak, while the soft-matter quasicrystals belong to a complex liquid between solid and liquid, whose fluid effect is very strong. This is a major difference between the solid and the soft-matter quasicrystals.

At an earlier period due to the lack of the equation of state, we have to compute by using $\rho = \text{const}$, in that case the computation on fluid field and mass density cannot be exactly determined, the present work has improved the situation, we add the state equation, and the field variables p and ρ can be exactly determined. It shows that the equation of state suggested in [1] is most important for the dynamics. However, the equation of state should be verified further by experiments.

The computation is stable, and it shows the solvability of the equations; the well conditionality of the formulation on the initial boundary value problem of the equations. All field variables through the specimen are determined numerically, including the important hydrodynamic variables: fluid pressure p in Figure 4 and mass density ρ in Figure 3(a). This

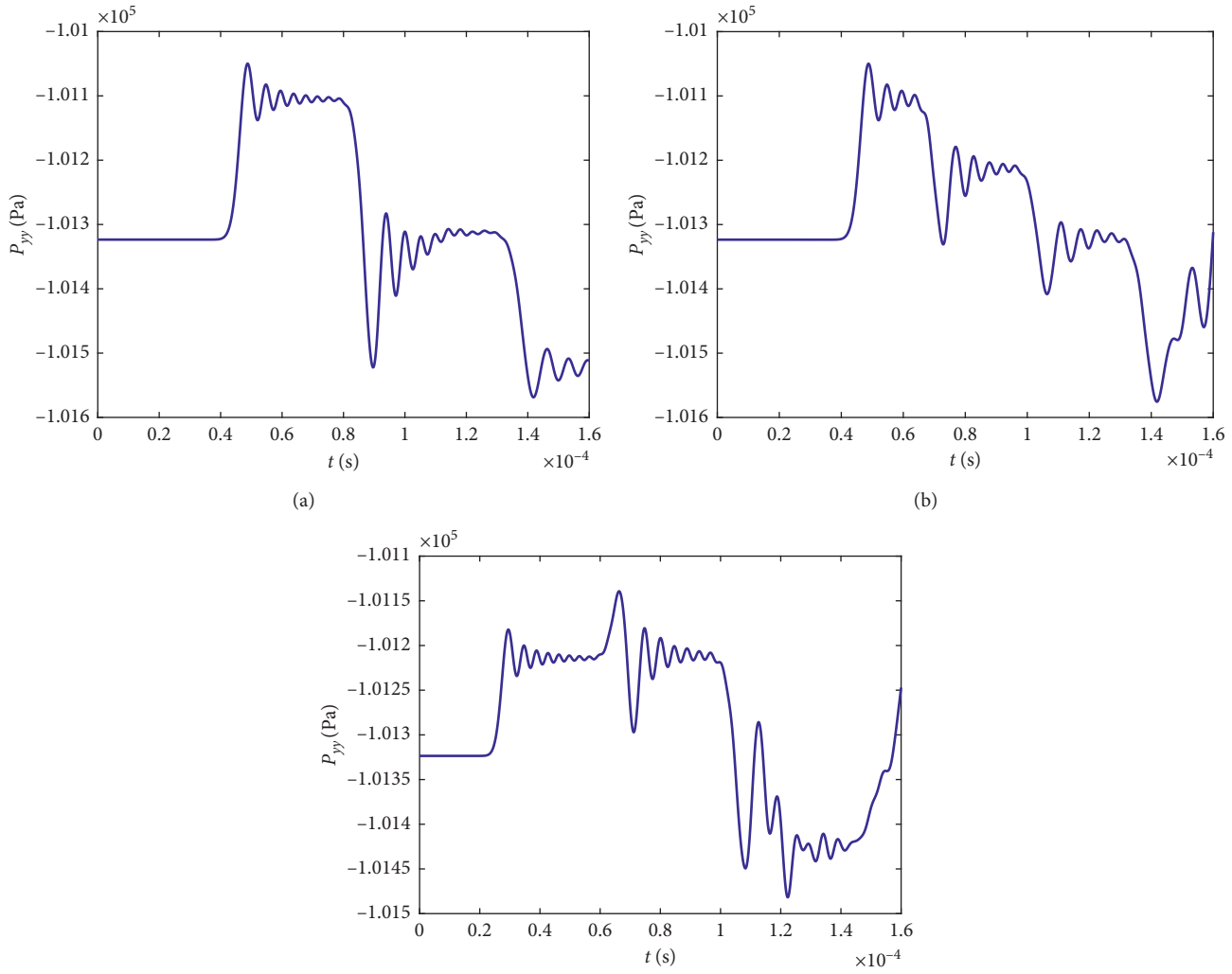

Figure 6: Normal stress of fluid field versus time (a) at the point A_1 (or A_2) of the specimen; (b) at the point A_3 (or A_4) 2 mm from A_1 (or A_2) towards the right in the horizontal direction; (c) at the point A_8 (or A_9) 2 mm from A_1 (or A_7) up in the perpendicular direction, reprinted from [11], copyright 2017 with permission from Springer Nature.

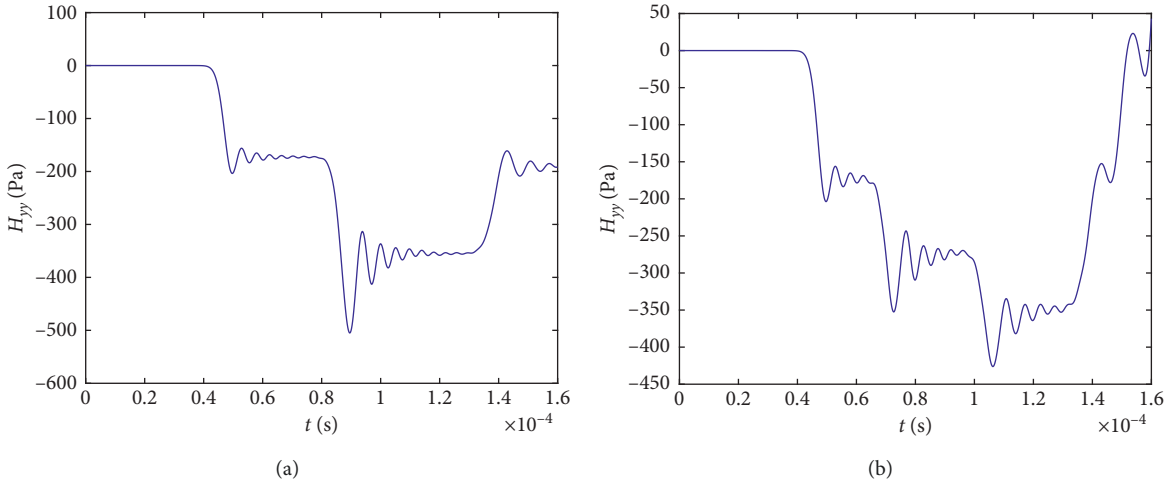

Figure 7: Continued.

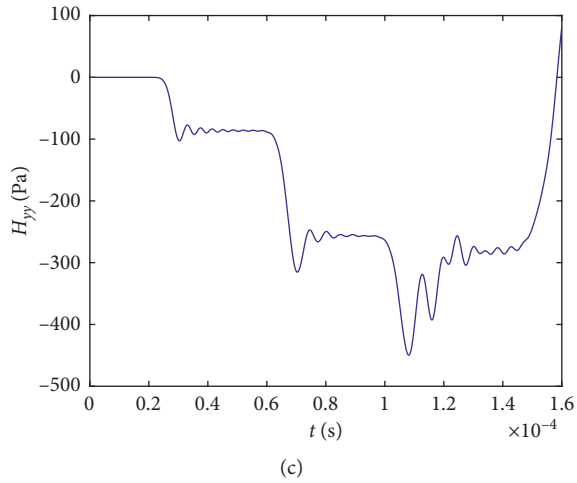

(c)

FIGURE 7: Normal stress of phason field versus time (a) at the point A_1 (or A_2) of the specimen; (b) at the point A_3 (or A_4) 2 mm from A_1 (or A_2) towards the right in the horizontal direction; (c) at the point A_8 (or A_9) 2 mm from A_1 (or A_7) up in the perpendicular direction, reprinted from [11], copyright 2017 with permission from Springer Nature.

improves the computational results, especially those related with fluid field.

Figure 3(b) shows the time variation of $\delta\rho/\rho$ is about in the order of magnitude 10^{-3} and 10 orders of magnitude higher than that (in the order of magnitude 10^{-13}) of solid quasicrystals [12]. These computational results indicate that the hydrodynamics of soft-matter quasicrystals is quite different from that of solid quasicrystals.

3. Sample II, Flow of Soft-Matter Quasicrystals Past a Circular Cylinder

3.1. Statement of the Problem. That sample I in Section 2 introduced is only one type of motion of the matter and of which there are other types. We here discuss another interesting case that the soft-matter quasicrystals flow past an obstacle, for example, a circular cylinder, shown in Figure 8, and the governing equation (1) should be modified as the generalized Oseen equations. But for simplicity, we here consider only the steady dynamics, so the terms of time derivative in (1) are omitted.

Suppose a slow flow along the direction x with the velocity U_∞ shown in Figure 8, the pressure p_∞ at infinity is omitted here, and the circular cylinder in an infinite soft-matter quasicrystal. We have the boundary conditions in the circular cylindrical coordinate system (r, θ, z):

$$\begin{aligned} &r = \sqrt{x^2 + y^2 + z^2} \longrightarrow \infty :\\ &V_r = U_\infty \cos\theta, V_\theta = -U_\infty \sin\theta, \sigma_{rr} = \sigma_{\theta\theta} = 0,\\ &\quad H_{rr} = H_{\theta\theta} = 0,\\ &r = a :\\ &V_r = V_\theta = 0, \sigma_{rr} = \sigma_{r\theta} = 0, H_{rr} = H_{r\theta} = 0. \end{aligned} \tag{4}$$

It is well known that, in the classical incompressible fluid dynamics, there was a famous work given by Oseen [17, 18] who overcame the well-known Stokes paradox. The key was modifying the Navier–Stokes equations, i.e., the Navier–Stokes equations of two-dimensional viscous fluid dynamics were revised as follows:

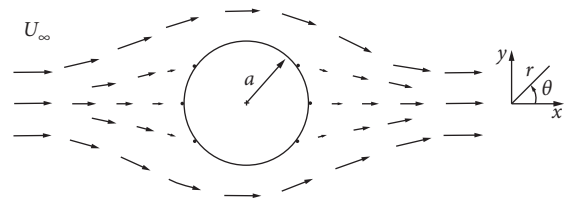

FIGURE 8: Flow of soft-matter quasicrystal past a circular cylinder with the radius a, reprinted from ref. [11], copyright 2017 with permission from Springer Nature.

$$\left.\begin{aligned} &\frac{\partial\rho}{\partial t} + \nabla\cdot(\rho\mathbf{V}) = 0,\\ &\frac{\partial(\rho V_x)}{\partial t} + \frac{\partial(U_x\rho V_x)}{\partial x} + \frac{\partial(U_y\rho V_x)}{\partial y} = -\frac{\partial p}{\partial x} + \eta\nabla^2(\rho V_x)\\ &\quad + \frac{1}{3}\eta\frac{\partial}{\partial x}\nabla\cdot\mathbf{V},\\ &\frac{\partial(\rho V_y)}{\partial t} + \frac{\partial(U_x\rho V_y)}{\partial x} + \frac{\partial(U_y\rho V_y)}{\partial y} = -\frac{\partial p}{\partial y} + \eta\nabla^2(\rho V_y)\\ &\quad + \frac{1}{3}\eta\frac{\partial}{\partial y}\nabla\cdot\mathbf{V},\\ &p = f(\rho), \end{aligned}\right\} \tag{5}$$

where U_x and U_y are the given values of corresponding velocities in the boundary conditions, and this means that, in momentum conservation equations, part of velocity components are replaced by known functions; equation (4) is called the Oseen equations. According to this modification, people solved successfully the flow past cylinder and other two-dimensional obstacles. In the next section, we present an

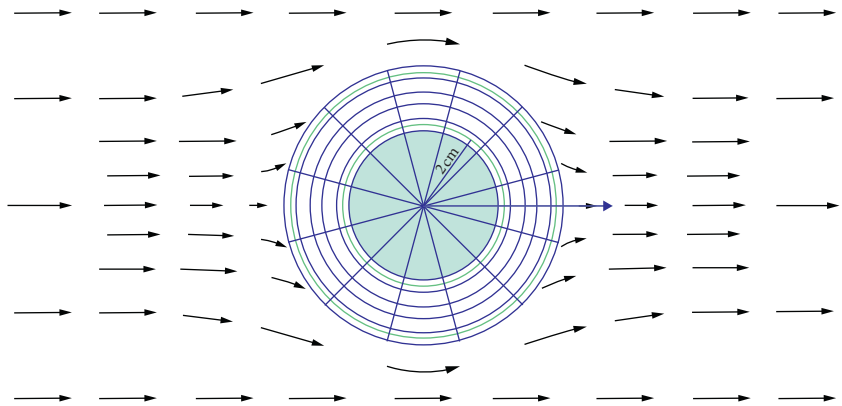

Figure 9: Finite difference grid in the polar coordinate system, reprinted from ref. [11], copyright 2017 with permission from Springer Nature.

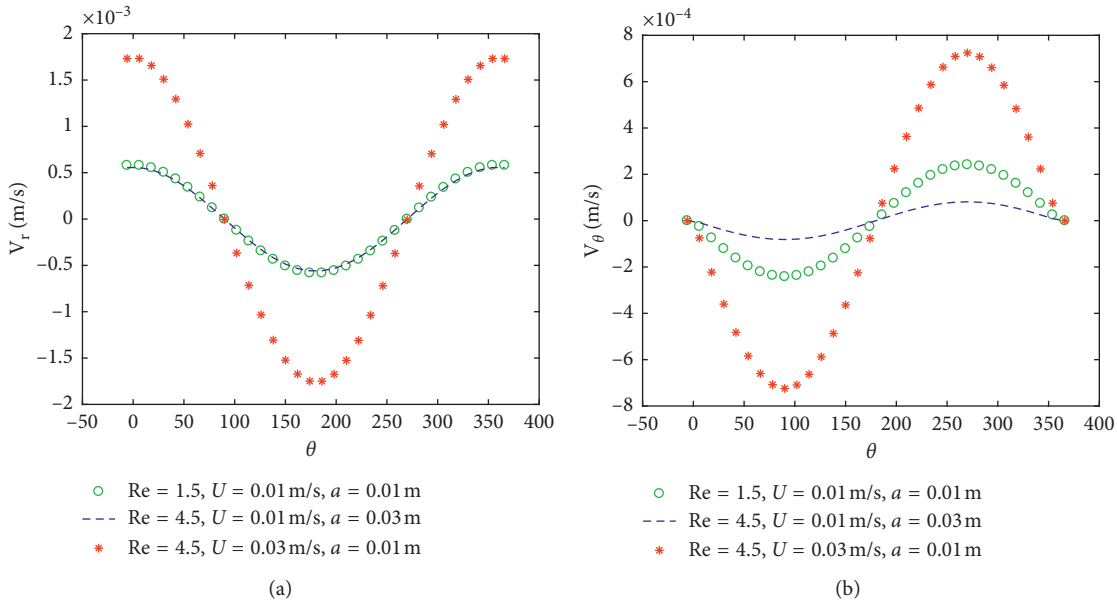

Figure 10: Angular distribution of velocity under different Reynolds number at $r = 1.55a$ and $t = 350\mu s$. (a) Radial velocity. (b) Circumferential velocity.

example about the applications. However, Oseen has studied only an incompressible viscous fluid past a cylinder; in this case, there is no need for an equation of state. Cheng and Fan, refer to Fan [11], developed the classical Oseen solution and studied a compressible viscous fluid past a cylinder, in which the equation of state is necessary, but this is only a numerical solution, named the generalized Oseen solution. At present, we have developed the work of Ref [11] and solved the flow of soft-matter quasicrystal with 8-fold symmetry past a cylinder, and the finite difference scheme is shown in Figure 9.

In the numerical analysis, the following material constants [11] $U_\infty = 0.01$ m/s, $\rho_0 = 1.5$ g/cm^3, $\eta = 1$ Poise, $l = 7 \sim 8$ nm, $r/a = 1.55$, $a = 1$ cm, $k_B = 1.38 \times 10^{-23}$ J/K, $T = 293$ K, $L = 10$ MPa, $M = 4$ MPa, $K_1 = 0.5$ L, $K_2 = -0.1$ L, $K_3 = 0.05$ L, $\Gamma_u = 4.8 \times 10^{-17}$ m^3·s/kg, $\Gamma_w = 4.8 \times 10^{-19}$ m^3·s/kg, $A \sim 0.2$ MPa, $B \sim 0.2$ MPa, and the phonon-phason coupling constant $R = 0.04$ M are used, and the computation is stable.

3.2. Numerical Results. A part of numerical results obtained are listed in the following through a series of illustrations. We find that among influence factors to the computational results the Reynolds number $\mathrm{Re} = \rho U_\infty a/\eta$ is most important. The variation of mass density versus time is shown in Figure 3(a). Here, we take the finite difference method to solve the present problem, and some results are given through the illustrations shown in Figures 10–13.

3.3. Analysis of Results. Figures 10–13 show the angular distribution of every kind of stress under different Reynolds

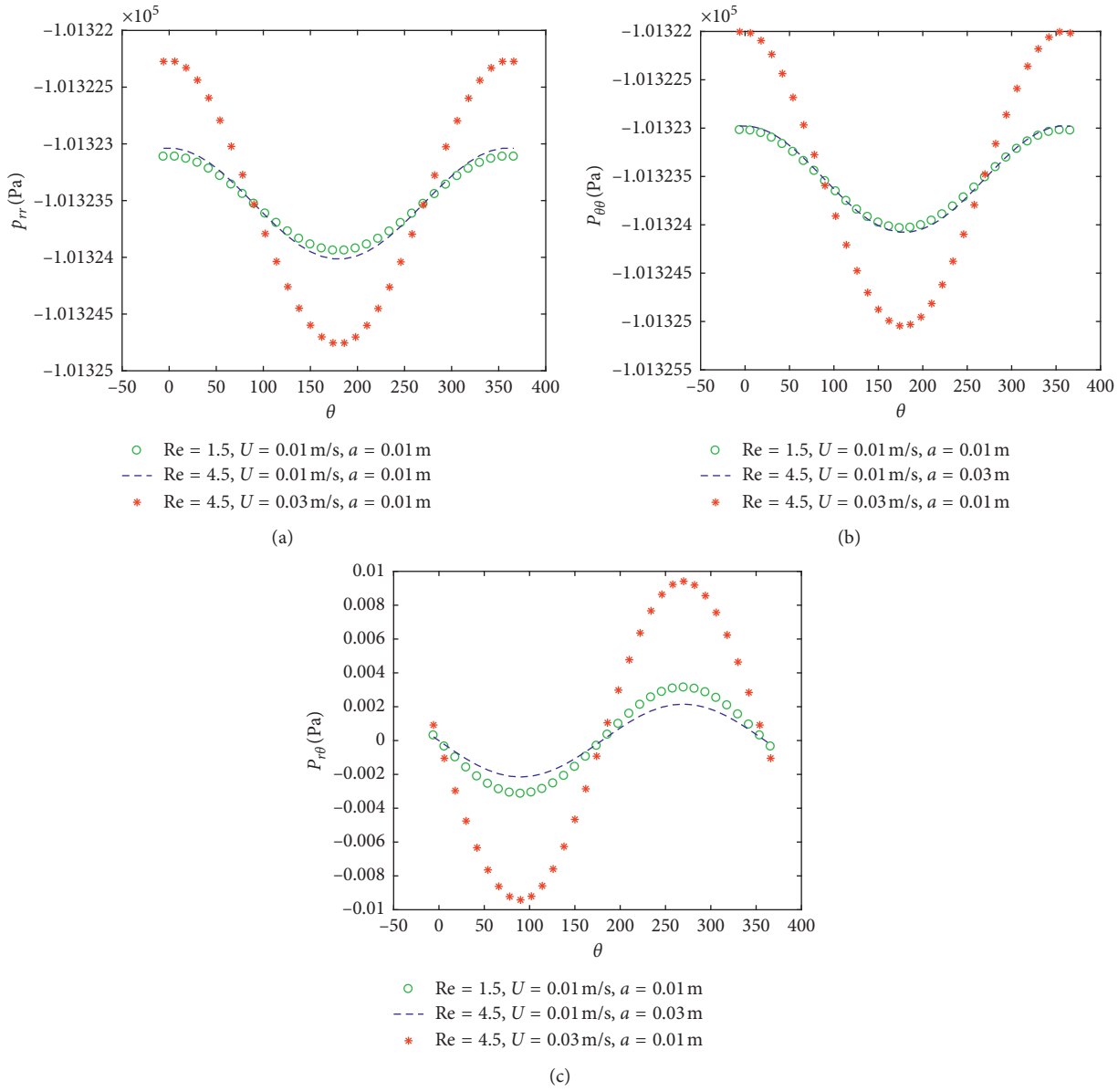

FIGURE 11: Angular distribution of normal stress, due to fluid viscosity under different Reynolds number, at $r = 3.55a$ and $t = 350\,\mu s$: (a) radial normal stress, (b) circumferential normal stress, and (c) shear stress $P_{r\theta}\,(P_{\theta r})$.

number, which explores the importance of degrees of freedom of phonons and phasons in quasicrystals.

Figures 10(a) and 10(b) show the angular distribution about radial and circumferential velocities under different Reynolds number. Due to the soft-matter, quasicrystals are influenced by the elementary excitation of phonons, phasons, and fluid phonons, so the magnitude of V_r and V_θ should be slower than the conventional liquid.

Figure 11 shows the angular distribution of normal stress of fluid phonon under different Reynolds number. The results are similar to the case of the 12-fold symmetry soft-matter quasicrystals. This is understandable since the two classes of quasicrystals both belong to the first kind of soft-matter quasicrystals, and they have very similar structures. The viscous fluid stress components are small, but total values of the normal stresses are quite considerable by adding the fluid pressure so that, for the soft-matter quasicrystals, fluid phonon and its effect are very important. This is the most evident distinction of soft-matter quasicrystals with the solid ones.

Figure 12 shows the angular distribution of normal stress of phonon under different Reynolds number. Also the results of 8-fold and 12-fold symmetry soft-matter quasicrystals are quite similar for the same reason. But the results of phonon are only for soft-matter quasicrystals, while there are no results of phonon for the conventional liquid as they have not the phonon elastic stresses.

More remarkable, contrast to 12-fold symmetry quasicrystals due to the decoupling between phonons and phasons in them, the 8-fold symmetry quasicrystals due to the

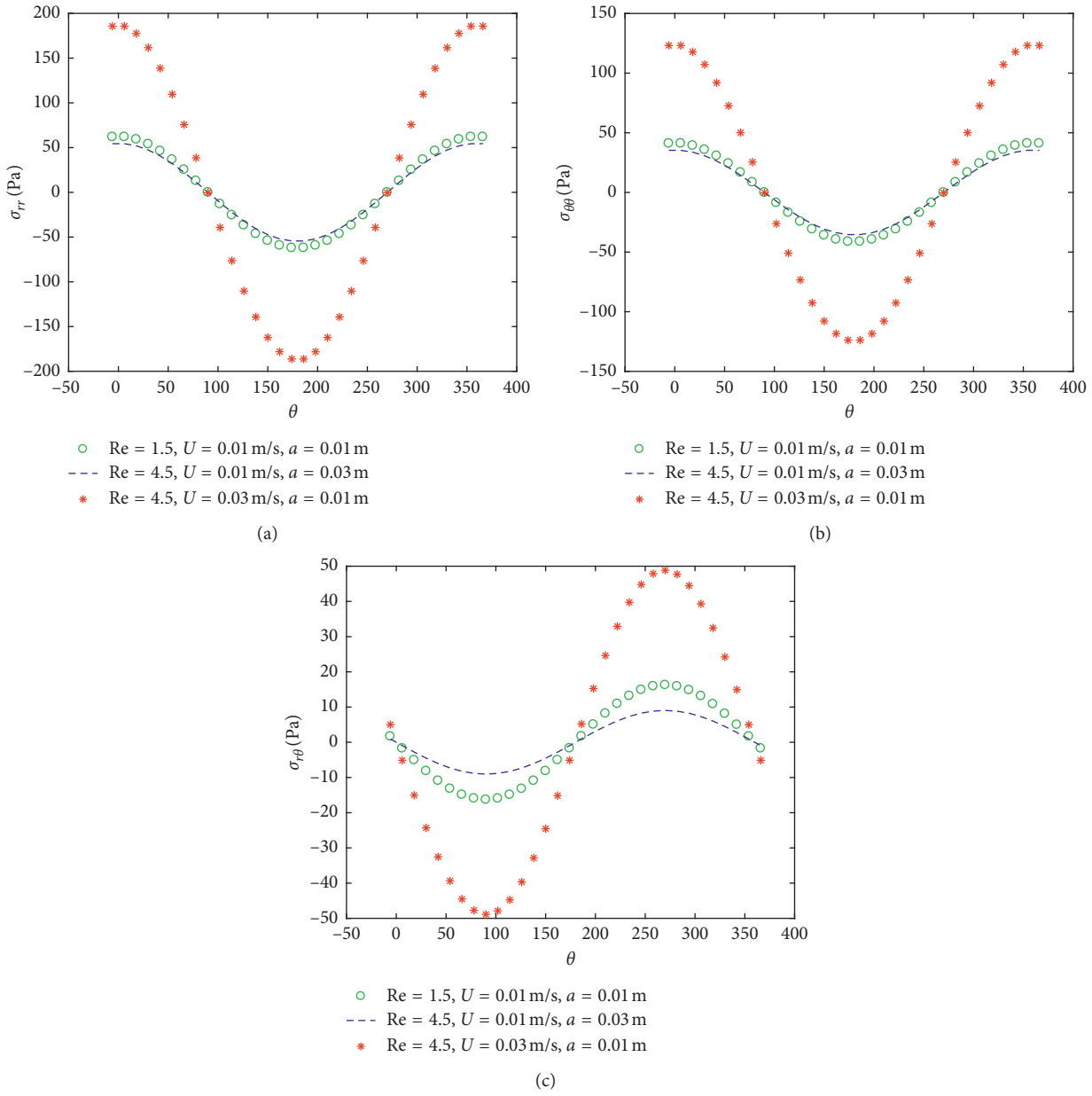

Figure 12: Angular distribution of normal stress of phonon under different Reynolds number at $r = 1.55a$ and $t = 350\,\mu s$: (a) radial normal stress, (b) circumferential normal stress, and (c) shear stress $\sigma_{r\theta}(\sigma_{\theta r})$.

coupling between phonons and phasons, of which the solution of phasons in Figure 13 is strongly exhibited. This is the main difference between the 8-fold and 12-fold soft-matter quasicrystals.

Another evident feature is that the Reynolds number is very important and influences the results largely. The above analysis show that all the results are under different Reynolds number, that is to say, at different flow velocity U_∞ and cylinder radius a.

The equation of state is important too; if there is not this equation then the basic equation set is not closed, there are no solutions.

The last but the most noteworthy feature is that the soft-matter quasicrystals are complex liquids, so they are very different from the conventional liquids. Compared the magnitudes of the results of soft-matter quasicrystals with the conventional liquids as shown in Ref [11] (see page 64 in chapter 6). The magnitude of the conventional liquids is 10^{-3} for radial velocity V_r, and the one of soft-matter quasicrystals in Figure 10(a) is also 10^{-3}, but the former is a little larger than the latter. In contrast to that, for circumferential velocity V_θ, the orders of magnitude of the former are 10^{-2}, while the ones of the latter are 10^{-4}, so the former are two times larger than the latter. This shows that the flow effect of the conventional liquids is stronger than the soft-matter quasicrystals which belong to a complex liquid between solid and liquid. Although there are some differences of the magnitudes in the results between the numerical solution for

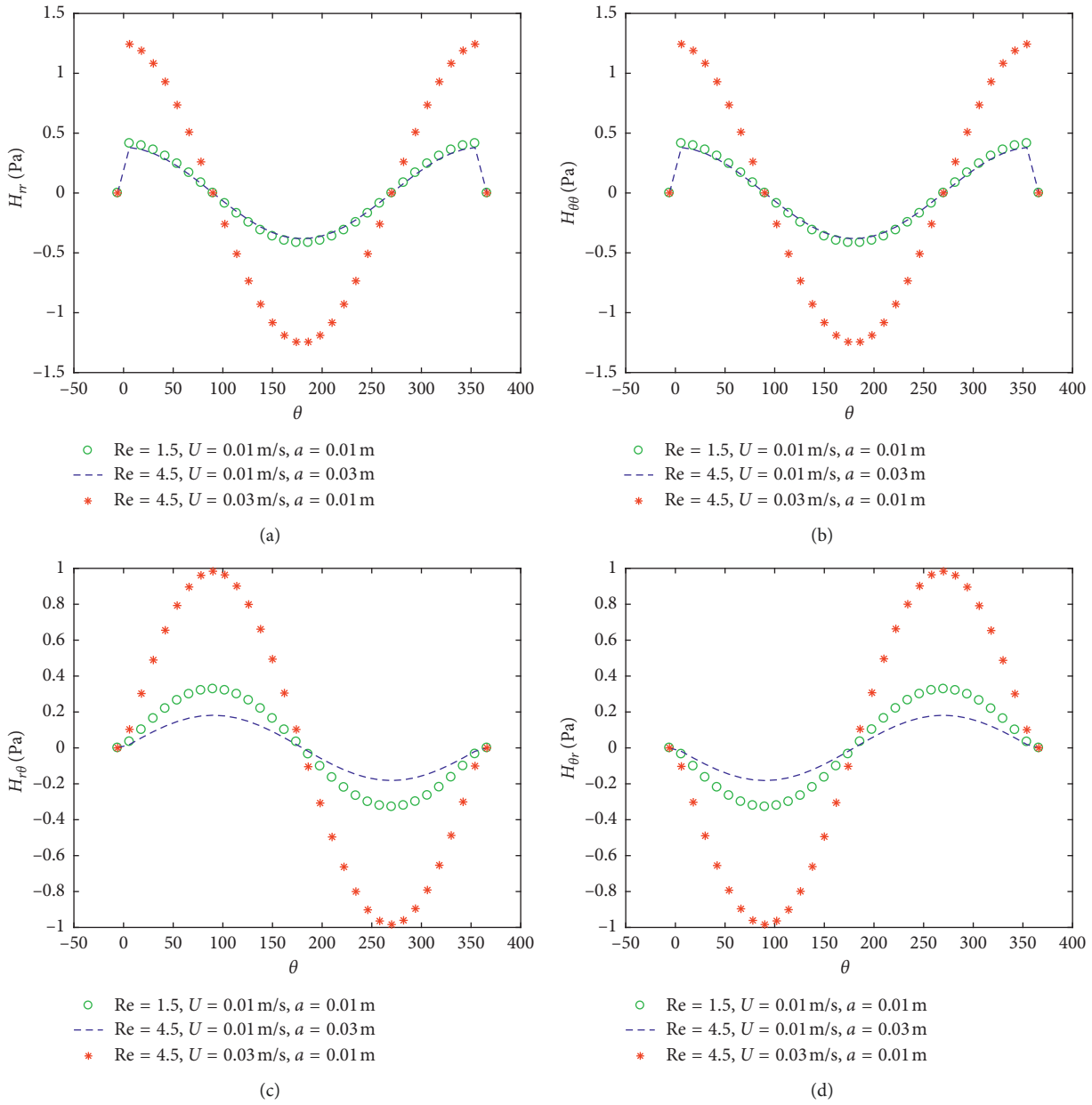

FIGURE 13: Angular distribution of the normal stress of phason under different Reynolds number at $r = 1.55a$ and $t = 350\,\mu s$: (a) radical normal stress, (b) circumferential normal stress, (c) shear stress $H_{r\theta}$, and (d) shear stress $H_{\theta r}$.

soft-matter quasicrystals and the Oseen solution for the conventional liquids, the structure of solutions is very similar. This verifies that the present model and method are correct and effective.

4. Conclusion and Discussion

A complete solution of equation set of hydrodynamics of possible soft-matter octagonal quasicrystals is constructed through the finite difference method. As computational examples, we have studied two different samples: one is a specimen under impact tension which is quite simple and can easily be tested experimentally and the other is the flow past a cylinder. The computation is systematical covering all hydrodynamic field variables, and the results verify the theory suggested in [1] and show the correctness of the formulation given in Section 2. The numerical procedure is very stable and is highly precise. In particular, the results reveal the nature of elementary excitations such as phonons, phasons, and fluid phonon; their interaction; and the gigantic differences in the physical behaviour between soft-matter and solid quasicrystals. For example, the compressibility of soft-matter quasicrystals is 10^{10} times greater than that of solid quasicrystals and the ratio P_{ij}/σ'_{ij} of the fluid stress of soft-matter quasicrystals over the viscous stress of the solid quasicrystals is 10^{15}. These great quantitative differences characterize qualitative differences of the dynamic nature between soft-matter and solid quasicrystals as well.

From the angle of generalized hydrodynamics of the complex system in Section 2, the present work is a heritage and development of hydrodynamics of solid quasicrystals of Lubensky et al. [8] which was derived by the Poisson bracket method, based on which Fan [1] derived the equation system of soft-matter quasicrystals, in which the key lies in that supplementation of the equation of state, which originated from Wensink [10]. The computation shows the nature of the intermediate phase between solid and fluid, so the equation system of soft-matter quasicrystals suggested in [1] is important, valid, and effective.

The analysis displayed in Section 3 explored the typical nature of soft matter of the material and exhibited once again the importance of the equation of state. The sample of the flow past cylinder in soft-matter quasicrystals with 8-fold symmetry reveals the fluid effect of the soft-matter quasicrystals and their effect is weaker than the conventional liquids, in which the Reynolds number plays an important role.

The work opens a field in dynamics of the soft-matter quasicrystal study and might be significant for other branches of soft matter science.

Appendix

The Constitutive Equations Relations

To solve the equations, we must give the constitutive equations and geometry gradient equations of deformation of the soft-matter quasicrystals in detail:

$$\begin{aligned}\sigma_{ij} &= \frac{\partial F}{\partial \varepsilon_{ij}} = C_{ijkl}\varepsilon_{kl} + R_{ijkl}w_{kl},\\ H_{ij} &= \frac{\partial F}{\partial w_{ij}} = K_{ijkl}w_{kl} + R_{klij}\varepsilon_{kl},\end{aligned} \tag{A.1}$$

where the function $F = F(\varepsilon_{ij}, w_{ij})$ is the elastic free energy density of the system with strain tensors for phonons and phasons:

$$\begin{aligned}\varepsilon_{ij} &= \frac{1}{2}\left(\frac{\partial u_i}{\partial x_j} + \frac{\partial u_j}{\partial x_i}\right),\\ w_{ij} &= \frac{\partial w_i}{\partial x_j},\end{aligned} \tag{A.2}$$

where C_{ijkl} is the phonon elastic constant tensor, K_{ijkl} is the phason elastic constant tensor, and R_{ijkl} is the phonon-phason coupling elastic constant tensor. For the fluid part of the stress tensor, there is

$$p_{ij} = -p\delta_{ij} + 2\eta\left(\dot{\xi}_{ij} - \frac{1}{3}\dot{\xi}_{kk}\delta_{ij}\right) + \zeta\dot{\xi}_{kk}\delta_{ij}, \tag{A.3}$$

with the deformation velocity tensor,

$$\dot{\xi}_{ij} = \frac{1}{2}\left(\frac{\partial V_i}{\partial x_j} + \frac{\partial V_j}{\partial x_i}\right), \tag{A.4}$$

where η is the first viscosity coefficient and ζ is the second one of the matter.

In order to make the closeness of the equation set, we must add an additional relation between pressure and mass density:

$$p = f(\rho), \tag{A.5}$$

which is often the named state equation and is given to equation (1) in the text.

In application to the 8-fold symmetry soft-matter quasicrystals, C_{ijkl} have only five nonzero and independent ones [16], i.e.,

$$\begin{aligned}&C_{1111} = C_{2222} = C_{11},\\ &C_{1122} = C_{12},\\ &C_{1212} = C_{1111} - C_{1122} = C_{11} - C_{12} = 2C_{66},\\ &C_{2323} = C_{3131} = C_{44},\\ &C_{1133} = C_{2233} = C_{13},\\ &C_{3333} = C_{33}.\end{aligned} \tag{A.6}$$

For the two-dimensional case, we have

$$\begin{aligned}&C_{ijkl} = L\delta_{ij}\delta_{kl} + M\left(\delta_{jk}\delta_{jl} + \delta_{il}\delta_{jk}\right), \quad i,j,k,l = 1,2,\\ &L = C_{12},\\ &M = \frac{(C_{11} - C_{12})}{2} = C_{66}.\end{aligned} \tag{A.7}$$

Also, applying the same to 12-fold symmetry quasicrystals, the phason elastic constant components are

$$\left.\begin{aligned}&K_{1111} = K_{2222} = K_1,\\ &K_{1122} = K_{2211} = K_2,\\ &K_{1221} = K_{2112} = K_3,\\ &K_{2121} = K_{1212} = K_1 + K_2 + K_3,\end{aligned}\right\} \tag{A.8}$$

and the others are zero. Equation (A.8) can also be expressed by

$$\begin{aligned}K_{ijkl} = {}&(K_1 - K_2 - K_3)(\delta_{ik} - \delta_{il}) + K_2\delta_{ij}\delta_{kl} + K_3\delta_{il}\delta_{jk}\\ &+ 2(K_2 + K_3)\left(\delta_{i1}\delta_{j2}\delta_{k1}\delta_{l2} + \delta_{i2}\delta_{j1}\delta_{k2}\delta_{l1}\right),\\ &i,j,k,l = 1,2.\end{aligned} \tag{A.9}$$

Due to the phonon-phason coupling for 8-fold symmetry quasicrystals, we have

$$\begin{aligned}&R_{1111} = R_{1122} = -R_{2222} = R_{1221} = R_{2121} = -R_{1212} = -R_{2121}\\ &\quad = R,\\ &R_{ijkl} = R(\delta_{i1} - \delta_{i2})\left(\delta_{ij}\delta_{kl} - \delta_{il}\delta_{jk} + \delta_{iljk}\right), \quad i,j,k,l = 1,2.\end{aligned} \tag{A.10}$$

For simplicity, only the scalar quantity form of η_{ijkl} is considered here, i.e.,

$$p_{ij} = -p\delta_{ij} + \eta\left(\dot{\xi}_{kl} - \frac{1}{3}\dot{\xi}_{kk}\delta_{ij}\right) + \zeta\dot{\xi}_{kk}\delta_{ij},$$
$$\dot{\xi}_{ij} = \frac{1}{2}\left(\frac{\partial V_i}{\partial x_j} + \frac{\partial V_j}{\partial x_i}\right), \quad \text{(A.11)}$$
$$\dot{\xi}_{kk} = \dot{\xi}_{11} + \dot{\xi}_{22} + \dot{\xi}_{33}.$$

where η is the first viscosity coefficient and ζ is the second one, but we put $\zeta = 0$ because its value is too small, also Γ_u and Γ_w denote the phonon and phason dissipation coefficients, and A and B are the material constants due to variation of mass density, respectively.

Data Availability

The data used to support the findings of this study are available from the corresponding author upon request.

Disclosure

A part of contents of the manuscript has been published in the book "Generalized Dynamics of Soft-Matter Quasicrystals: Mathematical Models and Solutions" by T. Y. Fan. The theory of the generalized dynamics is created by T. Y. Fan as the Ph. D. adviser of F. Wang.

Conflicts of Interest

The authors declare that they have no conflicts of interest.

Acknowledgments

This work was supported by the National Natural Science Foundation of China through grant 11272053. We thank Professor H. H. Wensink in Debye Institute of Utrecht University in Holland for the helpful discussion on the equation of state.

References

[1] T. Y. Fan, "Equation system of generalized hydrodynamics of soft-matter quasicrystals," *Journal of Applied Mathematics and Mechanics*, vol. 37, no. 4, pp. 331–347, 2016.

[2] X. Zeng, G. Ungar, Y. Liu, V. Percec, A. E. Dulcey, and J. K. Hobbs, "Supramolecular dendritic liquid quasicrystals," *Nature*, vol. 428, no. 6979, pp. 157–160, 2004.

[3] A. Takano, W. Kawashima, A. Noro et al., "A mesoscopic Archimedean tiling having a new complexity in an ABC star polymer," *Journal of Polymer Science Part B: Polymer Physics*, vol. 43, no. 18, pp. 2427–2432, 2005.

[4] K. Hayashida, T. Dotera, A. Takano, and Y. Matsushita, "Polymeric quasicrystal: mesoscopic quasicrystalline tiling in ABC star polymers," *Physical Review Letters*, vol. 98, no. 19, article 195502, 2007.

[5] D. V. Talapin, E. V. Shevchenko, M. I. Bodnarchuk, X. Ye, J. Chen, and C. B. Murray, "Quasicrystalline order in self-assembled binary nanoparticle superlattices," *Nature*, vol. 461, no. 7266, pp. 964–967, 2009.

[6] S. Fischer, A. Exner, K. Zielske et al., "Colloidal quasicrystals with 12-fold and 18-fold diffraction symmetry," *Proceedings of the National Academy of Sciences*, vol. 108, no. 5, pp. 1810–1814, 2011.

[7] K. Yue, M. Huang, R. Marson et al., "Geometry induced sequence of nanoscale Frank-Kasper and quasicrystal mesophases in giant surfactants," *Proceedings of the National Academy of Sciences*, vol. 113, no. 50, pp. 14195–14200, 2016.

[8] T. C. Lubensky, S. Ramaswamy, and J. Toner, "Hydrodynamics of icosahedral quasicrystals," *Physical Review B*, vol. 32, no. 11, pp. 7444–7452, 1985.

[9] E. M. Lifshitz and L. P. Petaevskii, *Statistical Physics, Part 2*, Butterworth-Heinemann, Oxford, UK, 1980.

[10] H. H. Wensink, "Equation of state of a dense columnar liquid crystal," *Physical Review Letters*, vol. 93, no. 15, article 157801, 2004.

[11] T. Y. Fan, *Generalized Dynamics of Soft-Matter Quasicrystals: Mathematical Models and Solutions (Chapter 7 and 9)*, Beijing Institute of Technology Press, Beijing, China/Springer-Verlag, Heidelberg, Germany, 2017.

[12] H. Cheng, T. Fan, and H. Wei, "Solutions for hydrodynamics of 5- and 10-fold symmetry quasicrystals," *Applied Mathematics and Mechanics*, vol. 37, no. 10, pp. 1393–1404, 2016.

[13] J. M. Keith, J. A. King, I. Miskioglu, and S. C. Roache, "Tensile modulus modeling of carbon-filled liquid crystal polymer composites," *Polymer Composites*, vol. 30, no. 8, pp. 1166–1174, 2009.

[14] P. G. De Gennes and J. Prost, *The Physics of Liquid Crystals*, Clarendon, Oxford, UK, 2nd edition, 1993.

[15] C. F. Soon, M. Youseffib, N. Blagden, and M. C. T. Denyera, "Influence of time dependent factors to the phases and Poisson's ratio of cholesteryl ester liquid crystals," *Journal of Science and Technology*, vol. 3, no. 1, pp. 1–14, 2011.

[16] T. Y. Fan, *Mathematical Theory of Elasticity of Quasicrystals and Its Applications*, Science Press, Beijing/Springer-Verlag, Heidelberg, Germany, 2nd edition, 2016.

[17] C. W. Oseen, "Ueber die Stokes'sche formel und ueber eine verwandte aufgabe in der hydrodynamik," *Ark Math Astronom Fys*, vol. 6, no. 29, pp. 1–20, 1910.

[18] C. W. Oseen, *Neuere Methoden und Ergibnisse in der Hydrodynamik*, Akademische Verlagsgesellschaft, Leipzig, Germany, 1927.